The Journal of Chemical Physics

Unphysical discontinuities, intruder states and regularization in *GW* methods

Cite as: J. Chem. Phys. **156**, 231101 (2022); https://doi.org/10.1063/5.0089317
Submitted: 24 February 2022 • Accepted: 25 May 2022 • Accepted Manuscript Online: 26 May 2022 • Published Online: 15 June 2022

Enzo Monino and Pierre-François Loos

The Journal of Chemical Physics | COMMUNICATION | scitation.org/journal/jcp

Unphysical discontinuities, intruder states and regularization in *GW* methods

Cite as: J. Chem. Phys. 156, 231101 (2022); doi: 10.1063/5.0089317
Submitted: 24 February 2022 • Accepted: 25 May 2022 •
Published Online: 15 June 2022

Enzo Monino and Pierre-François Loos[a)]

AFFILIATIONS

Laboratoire de Chimie et Physique Quantiques (UMR 5626), Université de Toulouse, CNRS, UPS, Toulouse, France

[a)]Author to whom correspondence should be addressed: loos@irsamc.ups-tlse.fr

ABSTRACT

By recasting the non-linear frequency-dependent *GW* quasiparticle equation into a linear eigenvalue problem, we explain the appearance of multiple solutions and unphysical discontinuities in various physical quantities computed within the *GW* approximation. Considering the *GW* self-energy as an effective Hamiltonian, it is shown that these issues are key signatures of strong correlation in the $(N \pm 1)$-electron states and can be directly related to the intruder state problem. A simple and efficient regularization procedure inspired by the similarity renormalization group is proposed to avoid such issues and speed up the convergence of partially self-consistent *GW* calculations.

I. INTRODUCTION

The *GW* approximation of many-body perturbation theory[1,2] allows us to compute accurately charged excitation (i.e., ionization potentials, electron affinities, and fundamental gaps) in solids and molecules.[3–6] Its popularity in the molecular electronic structure community is rapidly growing[7–30] because of its relatively low computational cost[31–35] and somehow surprising accuracy for weakly correlated systems.[19,21,22,30,36,37]

The idea behind the *GW* approximation is to recast the many-body problem into a set of non-linear one-body equations. The introduction of the self-energy Σ links the non-interacting Green's function G_0 to its fully interacting version G via the following Dyson equation:

$$G = G_0 + G_0 \Sigma G. \tag{1}$$

Electron correlation is then explicitly incorporated into one-body quantities via a sequence of self-consistent steps known as Hedin's equations.[1]

In recent studies,[38–42] we discovered that one can observe (unphysical) irregularities and/or discontinuities in the energy surfaces of several key quantities (ionization potential, electron affinity, fundamental and optical gaps, total and correlation energies, as well as excitation energies) even in the weakly correlated regime. These issues were discovered in Ref. 38 while studying a model two-electron system,[43–45] and they were further investigated in Ref. 39, where we provided additional evidences and explanations of these undesirable features in real molecular systems. In particular, we showed that each branch of the self-energy Σ is associated with a distinct quasiparticle solution, and that each switch between solutions implies a significant discontinuity in the quasiparticle energy due to the transfer of weight between two solutions of the quasiparticle equation.[39] Multiple solution issues in *GW* appear frequently[21,23,46] (even at finite temperature[47,48]), especially for orbitals that are energetically far from the Fermi level, such as in core ionized states[49,50] and finite-temperature schemes.

In addition to obvious irregularities in potential energy surfaces that hamper the accurate determination of properties such as equilibrium bond lengths and harmonic vibrational frequencies,[40,41] one direct consequence of these discontinuities is the difficulty to converge (partially) self-consistent *GW* calculations as the self-consistent procedure jumps erratically from one solution to the other even if convergence accelerator techniques such as DIIS[39,51,52] or more elaborate schemes[53] are employed. Note in passing that the present issues do not only appear in *GW* as the *T*-matrix[54–57] and second-order Green's function (or second Born) formalisms[58–68] exhibit the same drawbacks.

It was shown that these problems can be tamed by using a static Coulomb-hole plus screened-exchange (COHSEX)[1,69–71] self-energy[41] or by considering a fully self-consistent *GW*

scheme,[14,33,72–78] where one considers not only the quasiparticle solution but also the satellites at each iteration.[42] However, none of these solutions is completely satisfying as a static approximation of the self-energy can induce significant loss in accuracy and fully self-consistent calculations can be quite challenging in terms of implementation and cost.

In this paper, via an upfolding process of the non-linear *GW* equation,[79] we provide further physical insights into the origin of these discontinuities by highlighting, in particular, the role of intruder states. Inspired by regularized electronic structure theories,[80,81] these new insights allow us to propose a cheap and efficient regularization scheme in order to avoid these issues and speed up the convergence of partially self-consistent *GW* calculations.

Here, for the sake of simplicity, we consider the one-shot G_0W_0,[69,82–89] but the same analysis can be performed in the case of (partially) self-consistent schemes, such as evGW[69,89–92] (where one updates only the quasiparticle energies) and qsGW[7,93–97] (where both quasiparticle energies and orbitals are updated at each iteration). Moreover, we consider a Hartree–Fock (HF) starting point, but it can be straightforwardly extended to a Kohn–Sham starting point. Throughout this article, p and q are general (spatial) orbitals; i, j, k, and l denote occupied orbitals; a, b, c, and d are vacant orbitals; and m labels single excitations $i \to a$. Atomic units are used throughout.

II. DOWNFOLDING: THE NON-LINEAR *GW* PROBLEM

Within the G_0W_0 approximation, in order to obtain the quasiparticle energies and the corresponding satellites, one solve, for each spatial orbital p and assuming real values of the frequency ω, the following (non-linear) quasiparticle equation:

$$\epsilon_p^{\mathrm{HF}} + \Sigma_p^{\mathrm{c}}(\omega) - \omega = 0, \tag{2}$$

where ϵ_p^{HF} is the pth HF orbital energy, and the correlation part of the G_0W_0 self-energy is constituted by a hole (h) and a particle (p) term as follows:

$$\Sigma_p^{\mathrm{c}}(\omega) = \sum_{im} \frac{2(pi|m)^2}{\omega - \epsilon_i^{\mathrm{HF}} + \Omega_m^{\mathrm{RPA}}} + \sum_{am} \frac{2(pa|m)^2}{\omega - \epsilon_a^{\mathrm{HF}} - \Omega_m^{\mathrm{RPA}}}. \tag{3}$$

Within the Tamm–Dancoff approximation (that we enforce here for the sake of simplicity), the screened two-electron integrals are given by

$$(pq|m) = \sum_{ia} (pq|ia) X_{ia,m}^{\mathrm{RPA}}, \tag{4}$$

where Ω_m^{RPA} and $\boldsymbol{X}_m^{\mathrm{RPA}}$ are, respectively, the mth eigenvalue and eigenvector of the random-phase approximation (RPA) problem, i.e.,

$$\boldsymbol{A}^{\mathrm{RPA}} \cdot \boldsymbol{X}_m^{\mathrm{RPA}} = \Omega_m^{\mathrm{RPA}} \boldsymbol{X}_m^{\mathrm{RPA}}, \tag{5}$$

with

$$A_{ia,jb}^{\mathrm{RPA}} = (\epsilon_a^{\mathrm{HF}} - \epsilon_i^{\mathrm{HF}})\delta_{ij}\delta_{ab} + (ia|bj) \tag{6}$$

and

$$(pq|ia) = \iint \phi_p(\boldsymbol{r}_1)\phi_q(\boldsymbol{r}_1) \frac{1}{|\boldsymbol{r}_1 - \boldsymbol{r}_2|} \phi_i(\boldsymbol{r}_2)\phi_a(\boldsymbol{r}_2) d\boldsymbol{r}_1 d\boldsymbol{r}_2 \tag{7}$$

are two-electron integrals over the HF (spatial) orbitals $\phi_p(\boldsymbol{r})$. Because one must compute all the RPA eigenvalues and eigenvectors to construct the self-energy (3), the computational cost is $\mathcal{O}(O^3V^3) = \mathcal{O}(K^6)$, where O and V are the number of occupied and virtual orbitals, respectively, and $K = O + V$ is the total number of orbitals.

As a non-linear equation, Eq. (2) has many solutions $\epsilon_{p,s}^{\mathrm{GW}}$ (where the index s is numbering solutions) and their corresponding weights are given by the value of the following renormalization factor:

$$0 \leq Z_{p,s} = \left[1 - \left. \frac{\partial \Sigma_p^{\mathrm{c}}(\omega)}{\partial \omega} \right|_{\omega = \epsilon_{p,s}^{\mathrm{GW}}} \right]^{-1} \leq 1. \tag{8}$$

In a well-behaved case, one of the solution (the so-called quasiparticle) ϵ_p^{GW} has a large weight Z_p. Note that we have the following important conservation rules:[98–100]

$$\sum_s Z_{p,s} = 1, \quad \sum_s Z_{p,s} \epsilon_{p,s}^{GW} = \epsilon_p^{\mathrm{HF}}, \tag{9}$$

which physically shows that the mean-field solution of unit weight is "scattered" by the effect of correlation in many solutions of smaller weights.

In standard *GW* calculations in solids,[2] one assigns a quasiparticle peak to the solution of the Dyson equation (1) that is associated with the largest value of the spectral function,

$$S(\omega) = \frac{1}{\pi} |\operatorname{Im} G(\omega)|. \tag{10}$$

III. UPFOLDING: THE LINEAR *GW* PROBLEM

The non-linear quasiparticle equation (2) can be *exactly* transformed into a larger linear problem via an upfolding process where the 2h1p and 2p1h sectors are upfolded from the 1h and 1p sectors, respectively.[79,101–104] For each orbital p, this yields a linear eigenvalue problem of the form

$$\boldsymbol{H}^{(p)} \cdot \boldsymbol{c}^{(p,s)} = \epsilon_{p,s}^{GW} \boldsymbol{c}^{(p,s)}, \tag{11}$$

with

$$\boldsymbol{H}^{(p)} = \begin{pmatrix} \epsilon_p^{\mathrm{HF}} & \boldsymbol{V}_p^{\mathrm{2h1p}} & \boldsymbol{V}_p^{\mathrm{2p1h}} \\ (\boldsymbol{V}_p^{\mathrm{2h1p}})^\top & \boldsymbol{C}^{\mathrm{2h1p}} & \boldsymbol{0} \\ (\boldsymbol{V}_p^{\mathrm{2p1h}})^\top & \boldsymbol{0} & \boldsymbol{C}^{\mathrm{2p1h}} \end{pmatrix}, \tag{12}$$

where

$$C_{ija,kcl}^{\mathrm{2h1p}} = \left[(\epsilon_i^{\mathrm{HF}} + \epsilon_j^{\mathrm{HF}} - \epsilon_a^{\mathrm{HF}})\delta_{jl}\delta_{ac} - 2(ja|cl) \right] \delta_{ik}, \tag{13}$$

$$C_{iab,kcd}^{\mathrm{2p1h}} = \left[(\epsilon_a^{\mathrm{HF}} + \epsilon_b^{\mathrm{HF}} - \epsilon_i^{\mathrm{HF}})\delta_{ik}\delta_{ac} + 2(ai|kc) \right] \delta_{bd}, \tag{14}$$

and the corresponding coupling blocks read

$$V^{2h1p}_{p,klc} = \sqrt{2}(pk|cl), \quad V^{2p1h}_{p,kcd} = \sqrt{2}(pd|kc). \tag{15}$$

The size of this eigenvalue problem is $1 + O^2V + OV^2 = \mathcal{O}(K^3)$, and it has to be solved for each orbital that one wishes to correct. Thus, this step scales as $\mathcal{O}(K^9)$ with conventional diagonalization algorithms. Note, however, that the blocks $\boldsymbol{C}^{2h1p}$ and $\boldsymbol{C}^{2p1h}$ do not need to be recomputed for each orbital. Of course, this $\mathcal{O}(K^9)$ scheme is purely illustrative and current state-of-the-art GW implementation scales as $\mathcal{O}(K^3)$ because of efficient contour deformation and density fitting techniques.[35,46,105]

It is crucial to understand that diagonalizing $\boldsymbol{H}^{(p)}$ [see Eq. (12)] is completely equivalent to solving the quasiparticle equation (2). This can be further illustrated by expanding the secular equation associated with Eq. (12),

$$\det[\boldsymbol{H}^{(p)} - \omega\mathbf{1}] = 0, \tag{16}$$

and comparing it with Eq. (2) by setting

$$\Sigma^c_p(\omega) = \boldsymbol{V}^{2h1p}_p \cdot \left(\omega\mathbf{1} - \boldsymbol{C}^{2h1p}\right)^{-1} \cdot \left(\boldsymbol{V}^{2h1p}_p\right)^\top + \boldsymbol{V}^{2p1h}_p \cdot \left(\omega\mathbf{1} - \boldsymbol{C}^{2p1h}\right)^{-1} \cdot \left(\boldsymbol{V}^{2p1h}_p\right)^\top, \tag{17}$$

where $\mathbf{1}$ is the identity matrix. Because the renormalization factor (8) corresponds to the projection of the vector $\boldsymbol{c}^{(p,s)}$ onto the reference (or internal) space, the weight of a solution (p,s) is given by the first coefficient of their corresponding eigenvector $\boldsymbol{c}^{(p,s)}$, i.e.,

$$Z_{p,s} = \left[c^{(p,s)}_1\right]^2. \tag{18}$$

One can see this downfolding process as the construction of a frequency-dependent effective Hamiltonian where the internal space is composed by a single Slater determinant of the 1h or 1p sector and the external (or outer) space by all the 2h1p and 2p1h configurations.[79,106,107] The main mathematical difference between the two approaches is that, by diagonalizing Eq. (12), one has direct access to the internal and external components of the eigenvectors associated with each quasiparticle and satellite, and not only their projection in the reference space as shown by Eq. (18).

The element ϵ^{HF}_p of $\boldsymbol{H}^{(p)}$ [see Eq. (12)] corresponds to the (approximate) relative energy of the $(N \pm 1)$-electron reference determinant (compared to the N-electron HF determinant), while the eigenvalues of the blocks $\boldsymbol{C}^{2h1p}$ and $\boldsymbol{C}^{2p1h}$, which are $\epsilon^{HF}_i - \Omega^{RPA}_m$ and $\epsilon^{HF}_a + \Omega^{RPA}_m$, respectively, provide an estimate of the relative energy of the 2h1p and 2p1h determinants. In some situations, one (or several) of these determinants from the external space may become of similar energy than the reference determinant, resulting in a vanishing denominator in the self-energy (3). Hence, these two diabatic electronic configurations may cross and form an avoided crossing, and this outer-space determinant may be labeled as an intruder state. As we shall see below, discontinuities, which are ubiquitous in molecular systems, arise in such scenarios.

IV. AN ILLUSTRATIVE EXAMPLE

In order to illustrate the appearance and the origin of these multiple solutions, we consider the hydrogen molecule in the 6-31G basis set, which corresponds to a two-electron system with four spatial orbitals (one occupied and three virtuals). This example was already considered in our previous work,[39] but here we provide further insights on the origin of the appearances of these discontinuities. The downfolded and upfolded G_0W_0 schemes have been implemented in the electronic structure package QuAcK,[108] which is freely available at https://github.com/pfloos/QuAcK. These calculations are based on restricted HF eigenvalues and orbitals. We denote as $|1\bar{1}\rangle$ the N-electron ground-state Slater determinant, where the orbital 1 is occupied by one spin-up and one spin-down electron. Similar notations will be employed for the $(N \pm 1)$-electron configurations.

In Fig. 1, we report the variation of the quasiparticle energies of the four orbitals as functions of the internuclear distance R_{H-H}. One can easily diagnose two problematic regions showing obvious discontinuities around $R_{H-H} = 1.2$ Å for the LUMO+1 ($p = 3$) and $R_{H-H} = 0.5$Å for the LUMO+2 ($p = 4$). As thoroughly explained in Ref. 39, if one relies on the linearization of the quasiparticle equation (2) to compute the quasiparticle energies, i.e., $\epsilon^{GW}_p \approx \epsilon^{HF}_p + Z_p\Sigma^c_p(\epsilon^{HF}_p)$, these discontinuities are transformed into irregularities as the renormalization factor cancels out the singularities of the self-energy.

Figure 2 shows the evolution of the quasiparticle energy, the energetically close-by satellites and their corresponding weights as functions of R_{H-H}. Let us first look more closely at the region around $R_{H-H} = 1.2$Å involving the LUMO+1 [Fig. 2 (left)]. As one can see, an avoided crossing is formed between two solutions of the quasiparticle equation ($s = 4$ and $s = 5$). Inspection of their corresponding eigenvectors reveals that the $(N+1)$-electron determinants principally involved are the reference 1p determinant $|1\bar{1}3\rangle$ and an excited $(N+1)$-electron determinant of configuration $|12\bar{2}\rangle$ that becomes lower in energy than the reference determinant for $R_{H-H} > 1.2$Å. By construction, the quasiparticle solution diabatically follows the reference determinant $|1\bar{1}3\rangle$ through the avoided crossing (thick lines in Fig. 2), which is precisely the origin of the energetic discontinuity.

A similar scenario is at play in the region around $R_{H-H} = 0.5$Å for the LUMO+2 [Fig. 2 (right)] but it now involves three solutions ($s = 5$, $s = 6$, and $s = 7$). The electronic configurations of the Slater

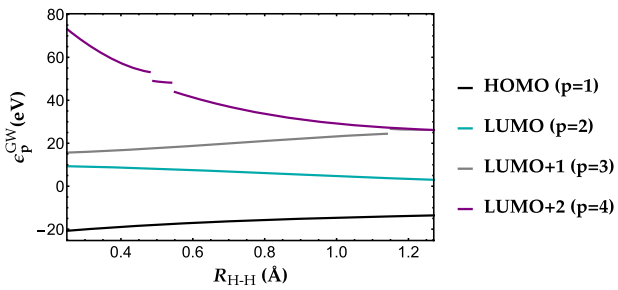

FIG. 1. Quasiparticle energies ϵ^{GW}_p as functions of the internuclear distance R_{H-H} (in Å) of H_2 at the G_0W_0@HF/6-31G level.

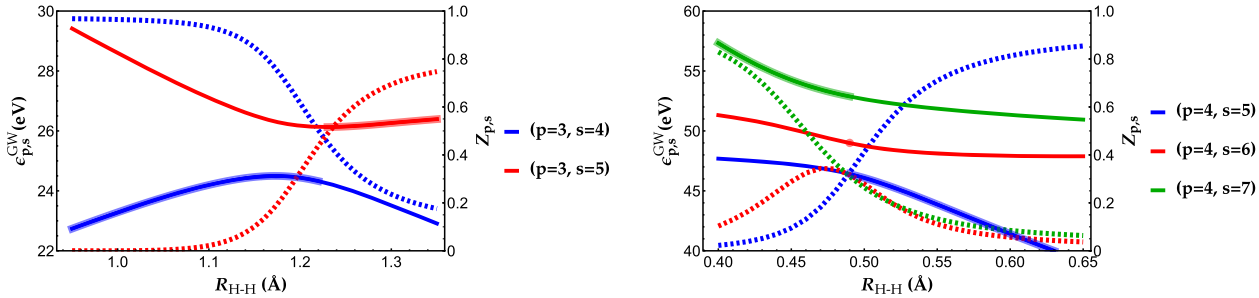

FIG. 2. Selection of quasiparticle and satellite energies $\epsilon^{GW}_{p,s}$ (solid lines) and their renormalization factor $Z_{p,s}$ (dashed lines) as functions of the internuclear distance R_{H-H} (in Å) for the LUMO+1 ($p = 3$) and LUMO+2 ($p = 4$) orbitals of H_2 at the G_0W_0@HF/6-31G level. The quasiparticle solution (which corresponds to the solution with the largest weight) is represented as a thicker line.

determinant involved are the $|1\bar{1}4\rangle$ reference determinant as well as two external determinants of configuration $|1\bar{2}3\rangle$ and $|12\bar{3}\rangle$. These states form two avoided crossings in rapid successions, which create two discontinuities in the energy surface (see Fig. 1). In this region, although the ground-state wave function is well described by the N-electron HF determinant, a situation that can be safely labeled as single-reference, one can see that the $(N+1)$-electron wave function involves three Slater determinants and can then be labeled as a multi-reference (or strongly correlated) situation with near-degenerate electronic configurations. Therefore, one can conclude that this downfall of GW is a key signature of strong correlation in the $(N \pm 1)$-electron states that yield a significant redistribution of weights among electronic configurations.

V. INTRODUCING REGULARIZED *GW* METHODS

One way to alleviate the issues discussed above and to massively improve the convergence properties of self-consistent GW calculations is to resort to a regularization of the self-energy without altering too much of the quasiparticle energies.

From a general perspective, a regularized GW self-energy reads

$$\tilde{\Sigma}^{c}_{p}(\omega;\eta) = \sum_{im} 2(pi|m)^2 f_\eta(\omega - \epsilon_i^{HF} + \Omega_m^{RPA}) + \sum_{am} 2(pa|m)^2 f_\eta(\omega - \epsilon_a^{HF} - \Omega_m^{RPA}), \quad (19)$$

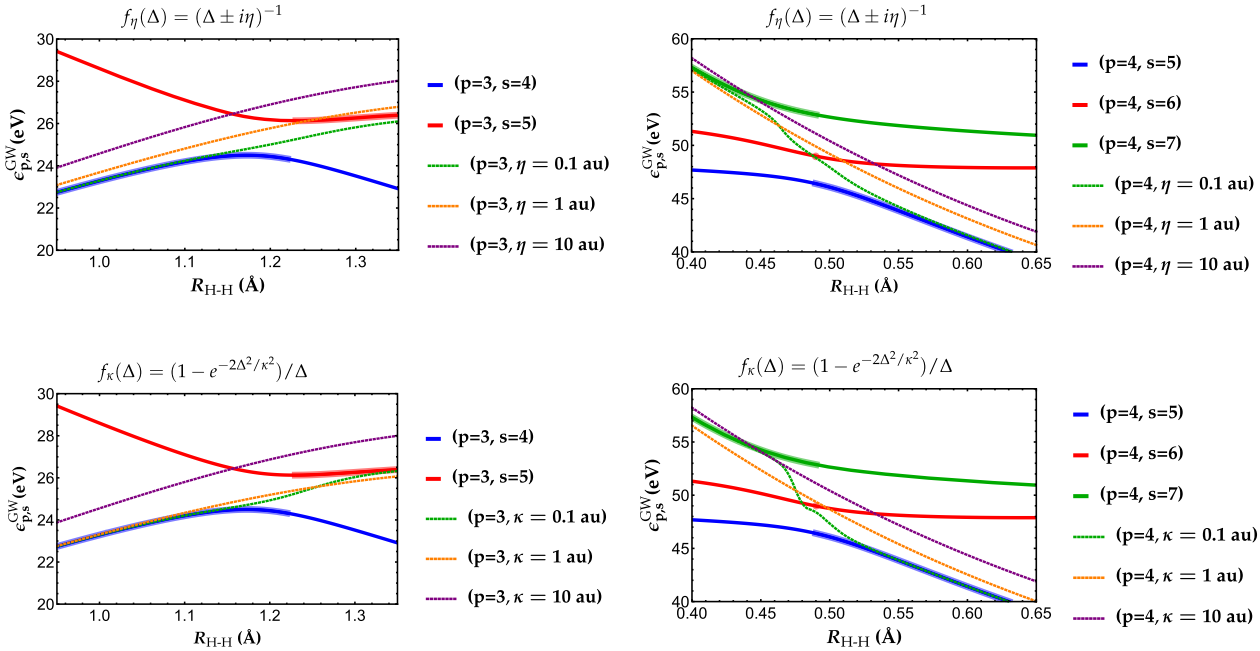

FIG. 3. Comparison between non-regularized (solid lines) and regularized (dashed lines) energies as functions of the internuclear distance R_{H-H} (in Å) for the LUMO +1 ($p = 3$) and LUMO+2 ($p = 4$) orbitals of H_2 at the G_0W_0@HF/6-31G level. The quasiparticle solution is represented as a thicker line.

where various choices for the "regularizer" f_η are possible. The main purpose of f_η is to ensure that $\tilde{\Sigma}_p^c(\omega;\eta)$ remains finite even if one of the denominators goes to zero. The regularized solutions $\tilde{\epsilon}_{p,s}^{GW}$ are then obtained by solving the following regularized quasiparticle equation:

$$\epsilon_p^{HF} + \tilde{\Sigma}_p^c(\omega;\eta) - \omega = 0. \tag{20}$$

Of course, by construction, one must have

$$\lim_{\eta\to 0}\tilde{\Sigma}_p^c(\omega;\eta) = \Sigma_p^c(\omega). \tag{21}$$

The most common and well-established way of regularizing Σ is via the simple energy-independent regularizer

$$f_\eta(\Delta) = (\Delta \pm i\eta)^{-1} \tag{22}$$

(with $\eta > 0$),[2,13,20,46] a strategy somehow related to the imaginary shift used in multiconfigurational perturbation theory.[109] Note that this type of broadening is customary in solid-state calculations; hence, such regularization is naturally captured in many codes.[2] In practice, an empirical value of η around 100 meV is suggested. Other choices are legitimate like the regularizers considered by Head-Gordon and coworkers within orbital-optimized second-order Møller–Plesset theory (MP2), which have the specificity of being energy-dependent.[80,110] In this context, the real version of the simple energy-independent regularizer (22) has been shown to damage thermochemistry performance and was abandoned.[111,112]

Our investigations have shown that the energy-dependent regularizer

$$f_\kappa(\Delta) = \frac{1 - e^{-2\Delta^2/\kappa^2}}{\Delta} \tag{23}$$

derived from the (second-order) perturbative analysis of the similarity renormalization group (SRG) equations[113–115] by Evangelista[116] is particularly convenient and effective for our purposes. Increasing κ gradually integrates out states with denominators Δ larger than κ, while the states with $\Delta \ll \kappa$ are not decoupled from the reference space, hence avoiding intruder state problems.[117]

Figure 3 compares the non-regularized and regularized quasiparticle energies in the two regions of interest for various η and κ values. It clearly shows how the regularization of the *GW* self-energy diabatically linked the two solutions to get rid of the discontinuities. However, this diabatization is more or less accurate depending on (i) the actual form of the regularizer and (ii) the value of η or κ.

Let us first discuss the simple energy-independent regularizer given by Eq. (22) [Fig. 3 (top)]. Mathematically, in order to link smoothly two solutions, the value of η has to be large enough so that the singularity lying in the complex plane at the avoided crossing is moved to the real axis (see Ref. 118 and references therein). This value is directly linked to the difference in energy between the two states at the avoided crossing and is thus, by definition, energy-dependent. This is clearly evidenced in Fig. 3 where, depending on the value of η, the regularization is more or less effective. For example, around $R_{H-H} = 1.1$Å (top-left), a value of 0.1 E_h (green curve) is appropriate, while at $R_{H-H} = 0.5$ Å (top-right), this value does not seem to be large enough. Note also that $\eta = 0.1E_h$ is significantly larger than the suggested value of 100 meV, and if one uses smaller η values, the regularization is clearly inefficient.

Let us now discuss the SRG-based energy-dependent regularizer provided in Eq. (23) [Fig. 3 (bottom)]. For $\kappa = 10E_h$, the value is clearly too large inducing a large difference between the two sets of quasiparticle energies (purple curves). For $\kappa = 0.1E_h$, we have the opposite scenario where κ is too small and some irregularities remain (green curves). We have found that $\kappa = 1.0E_h$ is a good compromise that does not alter significantly the quasiparticle energies while providing a smooth transition between the two solutions. Moreover, although the optimal κ is obviously system-dependent, this value performs well in all scenarios that we have encountered.

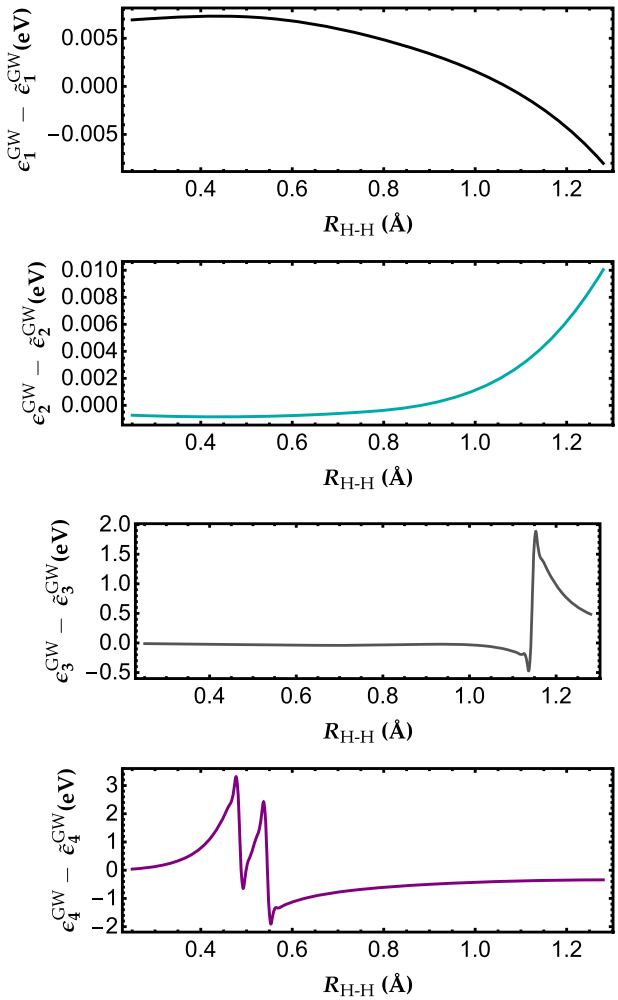

FIG. 4. Difference between regularized and non-regularized quasiparticle energies $\tilde{\epsilon}_p^{GW} - \epsilon_p^{GW}$ computed with $\kappa = 1.0E_h$ as functions of the internuclear distance R_{H-H} (in Å) of H_2 at the G_0W_0@HF/6-31G level. Similar graphs for $\kappa = 0.1E_h$ and $\kappa = 10E_h$ are provided in the supplementary material.

However, it can be certainly refined for specific applications. For example, in the case of regularized MP2 theory (where one relies on a similar energy-dependent regularizer), a value of $\kappa = 1.1$ has been found to be optimal for noncovalent interactions and transition metal thermochemistry.[110]

To further evidence this, Fig. 4 reports the difference between regularized (computed at $\kappa = 1.0E_h$ with the SRG-based regularizer) and non-regularized quasiparticle energies as functions of R_{H-H} for each orbital. The principal observation is that, in the absence of intruder states, the regularization induces an error below 10 meV for the HOMO ($p = 1$) and LUMO ($p = 2$), which is practically viable. Of course, in the troublesome regions ($p = 3$ and $p = 4$), the correction brought by the regularization procedure is larger (as it should), but it has the undeniable advantage to provide smooth curves. Similar graphs for $\kappa = 0.1E_h$ and $\kappa = 10E_h$ [and the simple regularizer given in Eq. (22)] are provided in the supplementary material, where one clearly sees that the larger the value of κ, the larger the difference between regularized and non-regularizer quasiparticle energies.

As a final example, we report in Fig. 5 the ground-state potential energy surface of the F_2 molecule obtained at various levels of theory with the cc-pVDZ basis. In particular, we compute, with and without regularization, the total energy at the Bethe–Salpeter equation (BSE) level[16,119–121] within the adiabatic connection fluctuation dissipation formalism[40,122,123] following the same protocol as detailed in Ref. 40. These results are compared to high-level coupled-cluster (CC) calculations extracted from the same work: CC with singles and doubles (CCSD)[124] and the non-perturbative third-order approximate CC method (CC3).[125] As already shown in Ref. 40, the potential energy surface of F_2 at the BSE@G_0W_0@HF (blue curve) is very "bumpy" around the equilibrium bond length

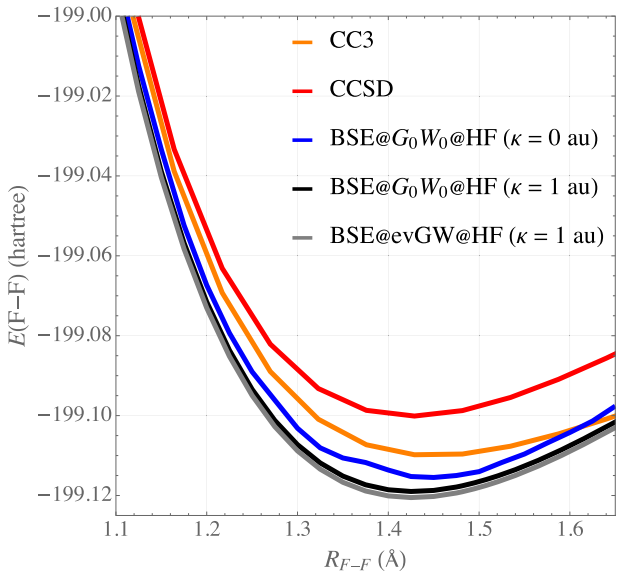

FIG. 5. Ground-state potential energy surface of F_2 around its equilibrium geometry obtained at various levels of theory with the cc-pVDZ basis set. Similar graphs for $\kappa = 0.1E_h$ and $\kappa = 10E_h$ are provided in the supplementary material.

and it is clear that the regularization scheme (black curve computed with $\kappa = 1.0E_h$) allows us to smooth it out without significantly altering the overall accuracy. Moreover, while it is extremely challenging to perform self-consistent *GW* calculations without regularization, it is now straightforward to compute the BSE@ev*GW*@HF potential energy surface (gray curve). For the sake of completeness, similar graphs for $\kappa = 0.1E_h$ and $\kappa = 10E_h$ are provided in the supplementary material. For $\kappa = 0.1E_h$, one still has issues. In particular, the BSE@ev*GW*@HF calculations do not converge for numerous values of the internuclear distance. Interestingly, for $\kappa = 10E_h$, the smooth BSE@G_0W_0@HF and BSE@ev*GW*@HF curves are superposed and of very similar quality as CCSD.

VI. CONCLUDING REMARKS

In this paper, we have provided mathematical and physical explanations behind the appearance of multiple solutions and discontinuities in various physical quantities computed within the *GW* approximation. More precisely, we have evidenced that intruder states are the main cause behind these issues and that this downfall of *GW* is a key signature of strong correlation. A simple and efficient regularization procedure inspired by the similarity renormalization group has been proposed to remove these discontinuities without altering too much the quasiparticle energies. Moreover, this regularization of the self-energy significantly speeds up the convergence of (partially) self-consistent *GW* methods. We hope that these new physical insights and technical developments will broaden the applicability of Green's function methods in the molecular electronic structure community and beyond.

SUPPLEMENTARY MATERIAL

See the supplementary material for the raw data associated with each figure as well as additional figures showing the effect of the regularizer and its parameter, with, in particular, the difference between non-regularized and regularized quasiparticle energies for H_2 and the ground-state potential energy surface of F_2 around its equilibrium geometry.

ACKNOWLEDGMENTS

The authors thank Pina Romaniello, Fabien Bruneval, and Xavier Blase for insightful discussions. This project has received funding from the European Research Council (ERC) under the European Union's Horizon 2020 Research and Innovation Programme (Grant Agreement No. 863481).

AUTHOR DECLARATIONS

Conflict of Interest

The authors have no conflicts to disclose.

DATA AVAILABILITY

The data that support the findings of this study are available within the article and its supplementary material.

REFERENCES

[1] L. Hedin, Phys. Rev. **139**, A796 (1965).
[2] R. M. Martin, L. Reining, and D. M. Ceperley, *Interacting Electrons: Theory and Computational Approaches* (Cambridge University Press, 2016).
[3] F. Aryasetiawan and O. Gunnarsson, Rep. Prog. Phys. **61**, 237 (1998).
[4] G. Onida, L. Reining, and A. Rubio, Rev. Mod. Phys. **74**, 601 (2002).
[5] L. Reining, Wiley Interdiscip. Rev. Comput. Mol. Sci. **8**, e1344 (2017).
[6] D. Golze, M. Dvorak, and P. Rinke, Front. Chem. **7**, 377 (2019).
[7] S.-H. Ke, Phys. Rev. B **84**, 205415 (2011).
[8] F. Bruneval, J. Chem. Phys. **136**, 194107 (2012).
[9] F. Bruneval and M. A. L. Marques, J. Chem. Theory Comput. **9**, 324 (2013).
[10] F. Bruneval, S. M. Hamed, and J. B. Neaton, J. Chem. Phys. **142**, 244101 (2015).
[11] X. Blase, P. Boulanger, F. Bruneval, M. Fernandez-Serra, and I. Duchemin, J. Chem. Phys. **144**, 034109 (2016).
[12] F. Bruneval, T. Rangel, S. M. Hamed, M. Shao, C. Yang, and J. B. Neaton, Comput. Phys. Commun. **208**, 149 (2016).
[13] F. Bruneval, J. Chem. Phys. **145**, 234110 (2016).
[14] P. Koval, D. Foerster, and D. Sánchez-Portal, Phys. Rev. B **89**, 155417 (2014).
[15] L. Hung, F. H. da Jornada, J. Souto-Casares, J. R. Chelikowsky, S. G. Louie, and S. Öğüt, Phys. Rev. B **94**, 085125 (2016).
[16] X. Blase, I. Duchemin, and D. Jacquemin, Chem. Soc. Rev. **47**, 1022 (2018).
[17] P. Boulanger, D. Jacquemin, I. Duchemin, and X. Blase, J. Chem. Theory Comput. **10**, 1212 (2014).
[18] J. Li, M. Holzmann, I. Duchemin, X. Blase, and V. Olevano, Phys. Rev. Lett. **118**, 163001 (2017).
[19] L. Hung, F. Bruneval, K. Baishya, and S. Öğüt, J. Chem. Theory Comput. **13**, 2135 (2017).
[20] M. J. van Setten, F. Weigend, and F. Evers, J. Chem. Theory Comput. **9**, 232 (2013).
[21] M. J. van Setten, F. Caruso, S. Sharifzadeh, X. Ren, M. Scheffler, F. Liu, J. Lischner, L. Lin, J. R. Deslippe, S. G. Louie, C. Yang, F. Weigend, J. B. Neaton, F. Evers, and P. Rinke, J. Chem. Theory Comput. **11**, 5665 (2015).
[22] M. J. van Setten, R. Costa, F. Viñes, and F. Illas, J. Chem. Theory Comput. **14**, 877 (2018).
[23] E. Maggio, P. Liu, M. J. van Setten, and G. Kresse, J. Chem. Theory Comput. **13**, 635 (2017).
[24] R. M. Richard, M. S. Marshall, O. Dolgounitcheva, J. V. Ortiz, J.-L. Brédas, N. Marom, and C. D. Sherrill, J. Chem. Theory Comput. **12**, 595 (2016).
[25] L. Gallandi, N. Marom, P. Rinke, and T. Körzdörfer, J. Chem. Theory Comput. **12**, 605 (2016).
[26] J. W. Knight, X. Wang, L. Gallandi, O. Dolgounitcheva, X. Ren, J. V. Ortiz, P. Rinke, T. Körzdörfer, and N. Marom, J. Chem. Theory Comput. **12**, 615 (2016).
[27] O. Dolgounitcheva, M. Díaz-Tinoco, V. G. Zakrzewski, R. M. Richard, N. Marom, C. D. Sherrill, and J. V. Ortiz, J. Chem. Theory Comput. **12**, 627 (2016).
[28] K. Krause, M. E. Harding, and W. Klopper, Mol. Phys. **113**, 1952 (2015).
[29] M. Govoni and G. Galli, J. Chem. Theory Comput. **14**, 1895 (2018).
[30] F. Caruso, M. Dauth, M. J. van Setten, and P. Rinke, J. Chem. Theory Comput. **12**, 5076 (2016).
[31] D. Foerster, P. Koval, and D. Sánchez-Portal, J. Chem. Phys. **135**, 074105 (2011).
[32] P. Liu, M. Kaltak, J. Klimeš, and G. Kresse, Phys. Rev. B **94**, 165109 (2016).
[33] J. Wilhelm, D. Golze, L. Talirz, J. Hutter, and C. A. Pignedoli, J. Phys. Chem. Lett. **9**, 306 (2018).
[34] A. Förster and L. Visscher, Front. Chem. **9**, 736591 (2021).
[35] I. Duchemin and X. Blase, J. Chem. Theory Comput. **17**, 2383 (2021).
[36] S. Körbel, P. Boulanger, I. Duchemin, X. Blase, M. A. L. Marques, and S. Botti, J. Chem. Theory Comput. **10**, 3934 (2014).
[37] F. Bruneval, N. Dattani, and M. J. van Setten, Front. Chem. **9**, 749779 (2021).
[38] P.-F. Loos, P. Romaniello, and J. A. Berger, J. Chem. Theory Comput. **14**, 3071 (2018).
[39] M. Véril, P. Romaniello, J. A. Berger, and P.-F. Loos, J. Chem. Theory Comput. **14**, 5220 (2018).
[40] P.-F. Loos, A. Scemama, I. Duchemin, D. Jacquemin, and X. Blase, J. Phys. Chem. Lett. **11**, 3536 (2020).
[41] J. A. Berger, P.-F. Loos, and P. Romaniello, J. Chem. Theory Comput. **17**, 191 (2020).
[42] S. Di Sabatino, P.-F. Loos, and P. Romaniello, Front. Chem. **9**, 751054 (2021).
[43] M. Seidl, Phys. Rev. A **75**, 062506 (2007).
[44] P. F. Loos and P. M. W. Gill, Phys. Rev. A **79**, 062517 (2009).
[45] P.-F. Loos and P. M. W. Gill, Phys. Rev. Lett. **103**, 123008 (2009).
[46] I. Duchemin and X. Blase, J. Chem. Theory Comput. **16**, 1742 (2020).
[47] P. Pokhilko and D. Zgid, J. Chem. Phys. **155**, 024101 (2021).
[48] P. Pokhilko, S. Iskakov, C.-N. Yeh, and D. Zgid, J. Chem. Phys. **155**, 024119 (2021).
[49] D. Golze, J. Wilhelm, M. J. van Setten, and P. Rinke, J. Chem. Theory Comput. **14**, 4856 (2018).
[50] D. Golze, L. Keller, and P. Rinke, J. Phys. Chem. Lett. **11**, 1840 (2020).
[51] P. Pulay, Chem. Phys. Lett. **73**, 393 (1980).
[52] P. Pulay, J. Comput. Chem. **3**, 556 (1982).
[53] P. Pokhilko, C.-N. Yeh, and D. Zgid, J. Chem. Phys. **156**, 094101 (2022).
[54] P. Romaniello, F. Bechstedt, and L. Reining, Phys. Rev. B **85**, 155131 (2012).
[55] D. Zhang, N. Q. Su, and W. Yang, J. Phys. Chem. Lett. **8**, 3223 (2017).
[56] J. Li, Z. Chen, and W. Yang, J. Phys. Chem. Lett. **12**, 6203 (2021).
[57] P.-F. Loos and P. Romaniello, J. Chem. Phys. **156**, 164101 (2022).
[58] A. Szabo and N. S. Ostlund, *Modern Quantum Chemistry* (McGraw Hill, New York, 1989).
[59] M. E. Casida and D. P. Chong, Phys. Rev. A **40**, 4837 (1989).
[60] M. E. Casida and D. P. Chong, Phys. Rev. A **44**, 5773 (1991).
[61] G. Stefanucci and R. van Leeuwen, *Nonequilibrium Many-Body Theory of Quantum Systems: A Modern Introduction* (Cambridge University Press, Cambridge, 2013).
[62] J. V. Ortiz, Wiley Interdiscip. Rev. Comput. Mol. Sci. **3**, 123 (2013).
[63] J. J. Phillips and D. Zgid, J. Chem. Phys. **140**, 241101 (2014).
[64] J. J. Phillips, A. A. Kananenka, and D. Zgid, J. Chem. Phys. **142**, 194108 (2015).
[65] A. A. Rusakov, J. J. Phillips, and D. Zgid, J. Chem. Phys. **141**, 194105 (2014).
[66] A. A. Rusakov and D. Zgid, J. Chem. Phys. **144**, 054106 (2016).
[67] S. Hirata, M. R. Hermes, J. Simons, and J. V. Ortiz, J. Chem. Theory Comput. **11**, 1595 (2015).
[68] S. Hirata, A. E. Doran, P. J. Knowles, and J. V. Ortiz, J. Chem. Phys. **147**, 044108 (2017).
[69] M. S. Hybertsen and S. G. Louie, Phys. Rev. B **34**, 5390 (1986).
[70] L. Hedin, J. Phys.: Condens. Matter **11**, R489 (1999).
[71] F. Bruneval, N. Vast, and L. Reining, Phys. Rev. B **74**, 045102 (2006).
[72] A. Stan, N. E. Dahlen, and R. v. Leeuwen, Europhys. Lett. **76**, 298 (2006).
[73] A. Stan, N. E. Dahlen, and R. van Leeuwen, J. Chem. Phys. **130**, 114105 (2009).
[74] C. Rostgaard, K. W. Jacobsen, and K. S. Thygesen, Phys. Rev. B **81**, 085103 (2010).
[75] F. Caruso, P. Rinke, X. Ren, M. Scheffler, and A. Rubio, Phys. Rev. B **86**, 081102(R) (2012).
[76] F. Caruso, D. R. Rohr, M. Hellgren, X. Ren, P. Rinke, A. Rubio, and M. Scheffler, Phys. Rev. Lett. **110**, 146403 (2013).
[77] F. Caruso, P. Rinke, X. Ren, A. Rubio, and M. Scheffler, Phys. Rev. B **88**, 075105 (2013).
[78] F. Caruso, "Self-consistent GW approach for the unified description of ground and excited states of finite systems," Ph.D. thesis, Freie Universität Berlin, 2013.
[79] S. J. Bintrim and T. C. Berkelbach, J. Chem. Phys. **154**, 041101 (2021).
[80] J. Lee and M. Head-Gordon, J. Chem. Theory Comput. **15**, 311 (2019).
[81] F. A. Evangelista, J. Chem. Phys. **141**, 054109 (2014).
[82] G. Strinati, H. J. Mattausch, and W. Hanke, Phys. Rev. Lett. **45**, 290 (1980).
[83] M. S. Hybertsen and S. G. Louie, Phys. Rev. Lett. **55**, 1418 (1985).
[84] R. W. Godby, M. Schlüter, and L. J. Sham, Phys. Rev. B **37**, 10159 (1988).
[85] W. von der Linden and P. Horsch, Phys. Rev. B **37**, 8351 (1988).
[86] J. Northrup, M. Hybertsen, and S. Louie, Phys. Rev. Lett. **66**, 500 (1991).
[87] X. Blase, X. Zhu, and S. G. Louie, Phys. Rev. B **49**, 4973 (1994).
[88] M. Rohlfing, P. Krüger, and J. Pollmann, Phys. Rev. B **52**, 1905 (1995).

[89]M. Shishkin and G. Kresse, Phys. Rev. B **75**, 235102 (2007).
[90]X. Blase and C. Attaccalite, Appl. Phys. Lett. **99**, 171909 (2011).
[91]C. Faber, C. Attaccalite, V. Olevano, E. Runge, and X. Blase, Phys. Rev. B **83**, 115123 (2011).
[92]T. Rangel, S. M. Hamed, F. Bruneval, and J. B. Neaton, J. Chem. Theory Comput. **12**, 2834 (2016).
[93]X. Gui, C. Holzer, and W. Klopper, J. Chem. Theory Comput. **14**, 2127 (2018).
[94]S. V. Faleev, M. van Schilfgaarde, and T. Kotani, Phys. Rev. Lett. **93**, 126406 (2004).
[95]M. van Schilfgaarde, T. Kotani, and S. Faleev, Phys. Rev. Lett. **96**, 226402 (2006).
[96]T. Kotani, M. van Schilfgaarde, and S. V. Faleev, Phys. Rev. B **76**, 165106 (2007).
[97]F. Kaplan, M. E. Harding, C. Seiler, F. Weigend, F. Evers, and M. J. van Setten, J. Chem. Theory Comput. **12**, 2528 (2016).
[98]P. C. Martin and J. Schwinger, Phys. Rev. **115**, 1342 (1959).
[99]G. Baym and L. P. Kadanoff, Phys. Rev. **124**, 287 (1961).
[100]G. Baym, Phys. Rev. **127**, 1391 (1962).
[101]O. J. Backhouse, M. Nusspickel, and G. H. Booth, J. Chem. Theory Comput. **16**, 1090 (2020).
[102]O. J. Backhouse and G. H. Booth, J. Chem. Theory Comput. **16**, 6294 (2020).
[103]O. J. Backhouse, A. Santana-Bonilla, and G. H. Booth, J. Phys. Chem. Lett. **12**, 7650 (2021).
[104]G. Riva, T. Audinet, M. Vladaj, P. Romaniello, and J. A. Berger, "Photoemission spectral functions from the three-body green's function," SciPost Phys. **12**, 093 (2022).
[105]I. Duchemin and X. Blase, J. Chem. Phys. **150**, 174120 (2019).
[106]M. Dvorak and P. Rinke, Phys. Rev. B **99**, 115134 (2019).
[107]M. Dvorak, D. Golze, and P. Rinke, Phys. Rev. Mat. **3**, 070801(R) (2019).
[108]P. F. Loos, "QuAcK: A software for emerging quantum electronic structure methods," https://github.com/pfloos/QuAcK, 2019.
[109]N. Forsberg and P.-Å. Malmqvist, Chem. Phys. Lett. **274**, 196 (1997).
[110]J. Shee, M. Loipersberger, A. Rettig, J. Lee, and M. Head-Gordon, J. Phys. Chem. Lett. **12**, 12084 (2021).
[111]D. Stück and M. Head-Gordon, J. Chem. Phys. **139**, 244109 (2013).
[112]R. M. Razban, D. Stück, and M. Head-Gordon, Mol. Phys. **115**, 2102 (2017).
[113]F. Wegner, Ann. Phys. **506**, 77 (1994).
[114]S. D. Glazek and K. G. Wilson, Phys. Rev. D **49**, 4214 (1994).
[115]S. R. White, J. Chem. Phys. **117**, 7472 (2002).
[116]F. A. Evangelista, J. Chem. Phys. **140**, 124114 (2014).
[117]C. Li and F. A. Evangelista, Annu. Rev. Phys. Chem. **70**, 245 (2019).
[118]A. Marie, H. G. A. Burton, and P.-F. Loos, J. Phys.: Condens. Matter **33**, 283001 (2021).
[119]E. E. Salpeter and H. A. Bethe, Phys. Rev. **84**, 1232 (1951).
[120]G. Strinati, Riv. Nuovo Cimento **11**, 1 (1988).
[121]X. Blase, I. Duchemin, D. Jacquemin, and P.-F. Loos, J. Phys. Chem. Lett. **11**, 7371 (2020).
[122]E. Maggio and G. Kresse, Phys. Rev. B **93**, 235113 (2016).
[123]C. Holzer, X. Gui, M. E. Harding, G. Kresse, T. Helgaker, and W. Klopper, J. Chem. Phys. **149**, 144106 (2018).
[124]G. D. Purvis III and R. J. Bartlett, J. Chem. Phys. **76**, 1910 (1982).
[125]O. Christiansen, H. Koch, and P. Jørgensen, J. Chem. Phys. **103**, 7429 (1995).